



Super resolving optical system based on spectral dilation

Zeev Zalevsky^{a,*}, Vardit Eckhouse^a, Naim Konforti^a, Amir Shemer^a,
David Mendlovic^a, Javier Garcia^b

^a Faculty of Engineering, Department of Physical Electronics, Tel Aviv University, 69978 Tel Aviv, Israel

^b Department d'Optica, Universitat de Valencia, D/Dr. Moliner 50, 46100 Burjassot, Valencia, Spain

Received 9 January 2003; received in revised form 23 April 2004; accepted 1 July 2004

Abstract

Time multiplexing is a common approach for achieving super resolution. The basic method involves moving two gratings one in front of the object and the other one in front of the camera. In this paper, we present a novel approach for obtaining super resolution not by shifting a grating, but by using its various dilations for obtaining the required encoding and decoding of information.

© 2004 Elsevier B.V. All rights reserved.

Keywords: Super resolution; Transfer function; Image formation

1. Background

The super resolution for one-dimensional objects may be implemented in several fields of science and industrial utilizations. The most common example for using such objects is for industrial scanners application where each product is marked by a one-dimensional bar code. This code contains fine details and needs to be resolved accurately in order to prevent false identification. Another example for one-dimensional

objects where super resolving abilities have significant urge may be seen in the microscopy field (particularly for medical applications). There, a three dimensional scanning is performed over a given tested sample. If super resolving approach is applied, the three dimensional scanning constraints may be converted to two-dimensional scanning. Such an improvement decreases the scanning time and reduces the system cost performance.

Every optical system can provide only a limited spatial resolution. In terms of spatial frequencies, the lens is band limited and functions as a low pass filter. The numerical aperture and the wavelength determine the cutoff frequency of the system.

* Corresponding author. Fax: +972 3 642 3508.
E-mail address: zzeev@eng.tau.ac.il (Z. Zalevsky).

Thus, an extension of the aperture may improve the spatial resolution of the optical system. However, physical extension is costly and not always possible. The purpose of super resolution is to obtain a synthetic enlargement of the aperture without changing its physical dimensions. The attempts to obtain effectively larger apertures follow a single principle. They are based on certain a priori knowledge about the object. The object should be approximately time independent [1–3], polarization independent [4], or mono-frequency (λ -independent) [5], one dimensional [6] or spatially restricted [7,8]. One of the most appealing approaches for achieving resolving power, which exceeds the classical limits, is related to temporally restricted objects and is based on two moving gratings [2]. The basic idea is to transmit, in several different temporal frequency bands the information about different spatial frequency bands. The first grating is placed in the input plane and is moving with velocity V . The moving grating is used to encode the spatial information of the object and to allow for its transmission throughout the limited aperture. At the output plane of the system another identical grating is placed. It moves along the opposite direction with the same velocity V , and its role is to decode the information passed throughout the aperture. The output is imaged onto a detector that acts as a time integrator. It was shown that this configuration is able to increase significantly the effective aperture of the system.

2. The presented approach

In the following experiment the encoding and decoding was done by spectral dilation and not by time shift. Instead of moving a grating with a constant velocity two masks M and M' were inserted in optically conjugate planes of the object and the image, respectively. The mask M in the object plane has grating characteristics. A simple Ronchi grating splits the incident wave into several diffraction orders, which illuminate the object under different angles of incidence and replicates the spatial spectrum of the object. This allows higher spatial frequencies to enter the system aper-

ture, but they are overlapped and so cannot be used to reconstruct the object. Both masks had varying periods in the x and y directions, which cause scaling in the Fourier plane. The scaling allows transmitting different spatial frequency bands in different angles, causing different spatial frequency bands to appear in different areas of the system aperture. Thus the scaling enables orthogonality, just as the various frequencies in the time multiplexing approach achieved due to the shifting of the grating mask. The orthogonality is achieved after averaging in the y -axis. The objective of the mask M' which is identical to mask M is to adjust the proper angular direction to all the encoded spectral bands which passed through the aperture. With this method after encoding and decoding the unwanted spectral information does not overlap with the desired spectral bands and thus it may be filtered out. In this paper, we present the following technique restricted to one-dimensional objects. The axis that has no information will be used for encoding and decoding of information to obtain the superresolution.

Section 3 presents a theoretical explanation about the principle behind the one-dimensional superresolution approach that was used in this experiment. Section 4 displays the experimental results. The paper is concluded in Section 5.

3. System analysis

In order to achieve superresolution by the method described in the introduction the optical set up shown in Fig. 1 was used.

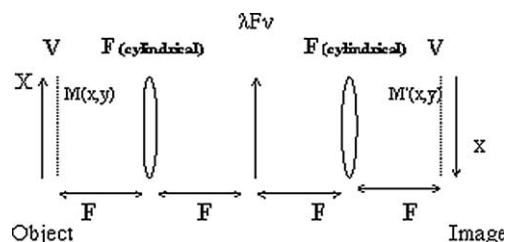


Fig. 1. Optical system for superresolution experiment by use of two masks M and M' .

The object and the mask (the encoder) that are adjacent in the optical set up are multiplied and then Fourier transformed by the first lens. This causes the desired scaling and shift of the spatial spectrum of the object into the narrow slit positioned at plane $Z = 2F$. This slit simulates the narrow aperture of the imaging lens. At $Z = 4F$ the output is multiplied by the second mask M' (the decoder) which replicates and scales the spectral information found at plane $Z = 2F$. Instead of using a low pass filter the amplitude in the image plane is spatially averaged in order to filter the unwanted spectral bands. The averaging is done digitally in the camera by summing all the pixels in the y -axis of the captured 2-D image and converting it to a 1-D image. This average is equivalent to an integral along the y -axis.

Let us now focus on the presented technique restricted to one-dimensional objects. Fig. 1 shows the optical configuration that was used for the system analysis. The masks M and M' have a varying period in the x and y directions, and are of the following type:

$$M(x, y) = \frac{1}{2} + \frac{1}{2} \cos \left[\frac{2\pi xy}{a} \right], \tag{1}$$

where a has units of square length and is the scaling factor. Note that actually the chosen mask presents a large number of 1-D (along x -axis) gratings that exhibit dilated frequency along the y -coordinate.

The input object is assumed to be illuminated by both spatially and temporally coherent light, so the mathematical analysis is performed with optical amplitudes. The field amplitude at $Z = 0$ is denoted by $E_0(x)$. The amplitude distribution just after the first mask is

$$\begin{aligned} E_0(x)M(x, y) &= \frac{1}{2}E_0(x) + \frac{1}{4}E_0(x) \exp \left[-\frac{2j\pi xy}{a} \right] \\ &\quad + \frac{1}{4}E_0(x) \exp \left[\frac{2j\pi xy}{a} \right] \\ &= U_0(x, y). \end{aligned} \tag{2}$$

Using a one-dimensional spatial Fourier transform operation, one can write the 1-D spatial spectrum of $U_0(x, y)$ at $Z = 2F$.

$$\begin{aligned} \hat{U}_0(v, y) &= \int U_0(x, y) \exp(-2\pi jvx) dx \\ &= \frac{1}{2}\tilde{E}_0(v) + \frac{1}{4}\tilde{E}_0\left(v - \frac{y}{a}\right) + \frac{1}{4}\tilde{E}_0\left(v + \frac{y}{a}\right), \end{aligned} \tag{3}$$

where $\tilde{E}_0(v)$ denotes the Fourier transform of $E_0(x)$. Eq. (3) shows how various scales of the encoding grating M were translated to shifts in the spectral domain. At $Z = 2F$ the system has a pupil function which for coherent light may be formulated as

$$\hat{P}_0(v) = \text{rect}\left(\frac{v}{\Delta v}\right) = \begin{cases} 1 & -\frac{\Delta v}{2} < v < \frac{\Delta v}{2}, \\ 0 & \text{else,} \end{cases} \tag{4}$$

where ‘rect’ is the rectangular function. The coherent transfer function for a rectangular aperture is drawn in Fig. 2.

At plane $Z = 4F$, just before the second mask M' , the amplitude distribution is

$$\begin{aligned} U(x', y') &= \int \hat{P}_0(v)\hat{U}_0(v, y') \exp(-2\pi jvx') dv \\ &= \int \left[\frac{1}{2}\tilde{E}_0(v) + \frac{1}{4}\tilde{E}_0\left(v - \frac{y'}{a}\right) \right. \\ &\quad \left. + \frac{1}{4}\tilde{E}_0\left(v + \frac{y'}{a}\right) \right] \text{rect}\left(\frac{v}{\Delta v}\right) \\ &\quad \times \exp(-2\pi jvx') dv, \end{aligned} \tag{5}$$

Eq. (5) is multiplied by the second identical mask M' yielding:

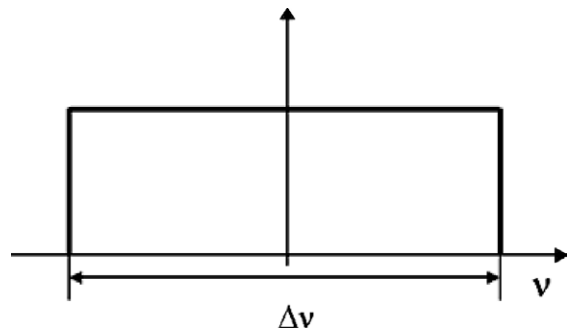


Fig. 2. Coherent transfer function for a rectangular aperture.

$$\begin{aligned}
U_1(x', y') &= U(x', y')M(x', y') \\
&= \left[\frac{1}{2} + \frac{1}{4} \exp\left(\frac{2\pi j x' y'}{a}\right) \right. \\
&\quad \left. + \frac{1}{4} \exp\left(\frac{-2\pi j x' y'}{a}\right) \right] \\
&\quad \times \int \left[\frac{1}{2} \tilde{E}_0(v) + \frac{1}{4} \tilde{E}_0\left(v - \frac{y'}{a}\right) \right. \\
&\quad \left. + \frac{1}{4} \tilde{E}_0\left(v + \frac{y'}{a}\right) \right] \text{rect}\left(\frac{v}{\Delta v}\right) \exp(-2\pi j v x') dv.
\end{aligned} \tag{6}$$

The distribution of Eq. (6) is imaged onto the CCD camera as shown in Fig. 1. Then the distribution is integrated along the y -axis to obtain the required decoding of the spatial spectral bands. After a few mathematical manipulations one obtains 9 terms that may be divide into 4 groups which have similar contributions to the final image (constant coefficients are not considered):

$$E(x') = E_1(x') + E_2(x') + E_3(x') + E_4(x'). \tag{7}$$

The first term is

$$\begin{aligned}
E_1(x') &= \int \tilde{E}_0(v) \text{rect}\left(\frac{v}{\Delta v}\right) \exp(-2\pi j x' v) dv \\
&\quad \times \int \exp\left(\frac{2\pi j x' y'}{a}\right) dy' \\
&= \delta(x') \int \tilde{E}_0(v) \text{rect}\left(\frac{v}{\Delta v}\right) \exp(-2\pi j x' v) dv \\
&= \text{const} \times \delta(x').
\end{aligned} \tag{8}$$

This term is a consequence of the multiplication of the second and the third term of the first brackets of Eq. (6) with the first term of the second brackets. Eq. (8) is a function that exists only in $X = 0$ and will have a very small impact on the reconstructed object.

The second term is

$$\begin{aligned}
E_2(x') &= \int \text{rect}\left(\frac{v}{\Delta v}\right) \exp(-2\pi j x' v) dv \\
&\quad \times \int \tilde{E}_0\left(v - \frac{y'}{a}\right) \exp\left(\frac{2\pi j x' y'}{a}\right) dy' \\
&= E_0(x') \int \text{rect}\left(\frac{v}{\Delta v}\right) \exp(-2\pi j x' v) \exp(2\pi j x' v) dv \\
&= \text{const} \times E_0(x').
\end{aligned} \tag{9}$$

This term is a consequence of the multiplication of the second and the third term of the first brackets of Eq. (6) with the second term of the second brackets. Eq. (9) is the reconstructed object $E_0(x')$ multiplied by a constant factor.

The third term is

$$\begin{aligned}
E_3(x') &= \int \text{rect}\left(\frac{v}{\Delta v}\right) \exp(-2\pi j x' v) dv \\
&\quad \times \int \tilde{E}_0\left(v + \frac{y'}{a}\right) \exp\left(\frac{2\pi j x' y'}{a}\right) dy' \\
&= E_0(x') \int \text{rect}\left(\frac{v}{\Delta v}\right) \exp(-2\pi j x' v) \\
&\quad \times \exp(-2\pi j x' v) dv \\
&= \text{PSF}\left(\frac{\Delta v x'}{2}\right) \times E_0(x').
\end{aligned} \tag{10}$$

This term is a consequence of the multiplication of the second and the third term of the first brackets of Eq. (6) with the third term of the second brackets. Eq. (10) is the reconstructed object multiplied by the Fourier transform of the pupil function (scaled by a factor of 2), which is very narrow around $X = 0$ in comparison with the image plane (around one half of the object's typical period).

The fourth term equals to:

$$\begin{aligned}
E_4(x') &= \int \text{rect}\left(\frac{v}{\Delta v}\right) \exp(-2\pi j x' v) dv \int \hat{U}_0(v, y') dy' \\
&= \text{LRI}(x') + \text{const} \times \text{PSF}(\Delta v x').
\end{aligned} \tag{11}$$

This term is a consequence of the multiplication of the first term of the first brackets of Eq. (6) with the terms of the second brackets. Eq. (11) is a Fourier transform of the pupil function which is again a very narrow function around $X = 0$ in the image plane (around one object's period) plus the low resolution image $\text{LRI}(x')$ that is obtained when the input is imaged through the limited aperture. Thus one may see in the image plane the reconstructed object E_0 (Eq. (9)) plus the narrow PSF function (Eq. (10)) plus the delta function (Eq. (8)) and the low resolution image (Eq. (11)). For instance observing the experimental results seen in Fig. 5(c) reveals bright line at the origins ($X = 0$). This line is the narrow PSF plus the delta function. In Fig. 5(d) the contrast of this line was

digitally decreased. Due to the used input which contains high spatial frequencies the influence of the LRI term is small since there is not much information in those low spatial frequencies and they are mainly expressed as low resolution background. Its subtraction improves the overall contrast of the image (i.e. see Fig. 5(d)).

4. Experimental results

Here this approach is demonstrated for one-dimensional superresolution where the axis that carries no information will be used for the different dilations. This approach can be applied for objects with a cigar shaped area in the spatial frequency domain that is badly matched to the frequency transfer domain of a lens. For experimental validation of the suggested approach, we used the set up shown in Fig. 3.

A He–Ne laser with a wavelength of 632.8 nm illuminated an object $E_0(x)$ and a mask M (attached to $E_0(x)$). The two masks M and M' have to be inserted in optical conjugate planes and have to be identical. The masks have to be perfectly aligned in order to achieve good results. One way to overcome this problem is to implement the second (decoding) mask using the computer that is connected to the CCD camera in the image plane. This can be done since the mask is an amplitude mask and not a phase mask. Before performing the experiment the mask M is imaged on the CCD camera with an open aperture, and saved on the computer. This image of mask M will be used instead of the mask M' . Then the CCD grabs the intensity in the image plane without the mask

M' . The computer that was connected to the CCD camera uses the stored (or generated) intensity mask M' and multiplies it with the intensity grabbed from the image plane. So we would have on the computer:

$$I = |E|^2 |M'|^2, \quad (12)$$

where E is the amplitude in the image plane before multiplication by M' and I is the intensity calculated by the computer. If a real mask M' was used, the CCD camera would have grabbed the intensity in the image plane which is the square of the multiplication between the amplitude of the image and the amplitude of the mask M' . This equals to the described by Eq. (12).

Since we used coherent light the summation would have to be over amplitudes and not intensities. Note that because the multiplication is done between the grabbed images in the computer it is possible to overcome this problem.

The readout of the CCD camera is related to the field distribution that illuminates it as: $|E|^{2\gamma}$. Thus in order to multiply amplitudes instead of intensities a root of 2γ should be applied to the captured images prior to the multiplication operation with the decoding mask. This could not have been done if the grabbed image was optically multiplied by the mask M' . The CCD camera we were using had $\gamma = 0.45$ so we applied a root of $1/0.9$ to the intensities readout that were grabbed by the camera before performing the multiplication. A slit with a width of $0.063F$ was placed in the Fourier plane to mimic a low performance imaging system. This means that for a coherent illumination periods smaller than $200 \mu\text{m}$ would not pass the imaging system. Another advantage of using

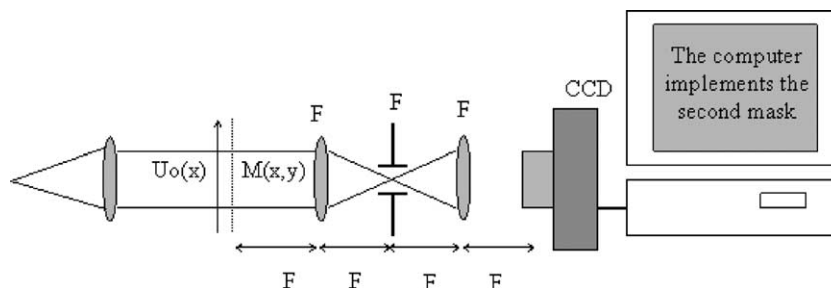


Fig. 3. Experimental setup.

a computer was that instead of using a low pass filter along the y -axis in the Fourier plane (in order to filter out the terms that do not resemble the object), after the multiplication the result was inte-

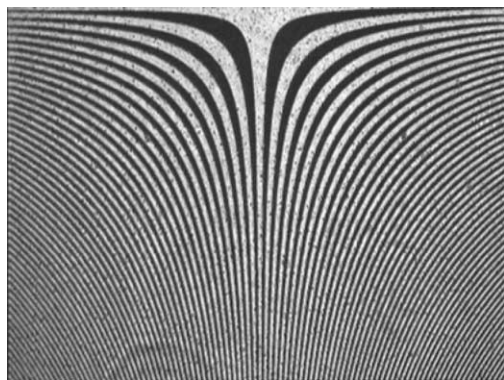


Fig. 4. Mask M and M' used in the setup with a period ranging from 0 to 100 μm .

grated over the y -axis. From the mathematics we expected a very narrow distortion of the image around $X=0$, we eliminated that by image processing since the image was grabbed and M' had a period ranging from 0 to 100 μm as can be seen in Fig 4. Fig. 5(a)–(d) are the results for the first input (chirp with period ranging from 200 to 450 μm): (a) is the original object imaged through the optical system with an open aperture, (b) is the object imaged through the low performance imaging system (close aperture), (c) is the object imaged through the optical system with a closed aperture, when masks M and M' are inserted and (d) is the object imaged through the closed aperture system with masks M and M' with image processing. As can be seen the object information, which was lost when, imaged through the closed aperture system was reconstructed after inserting masks M and M'. The image processing step contained filtering the narrow distortion in the optical axis and sub-

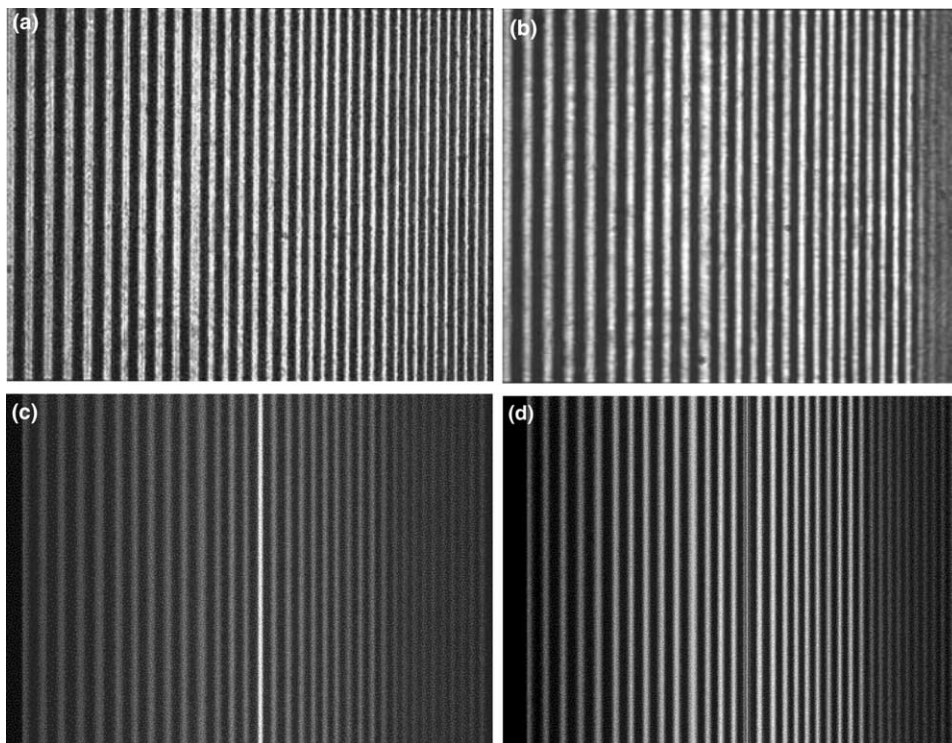


Fig. 5. Output (chirp with period ranging from 200 to 450 μm) captured by the CCD camera with (a) a clear aperture, (b) a closed aperture without the masks M and M', (c) a closed aperture with the masks M and M' without image processing and (d) with image processing.

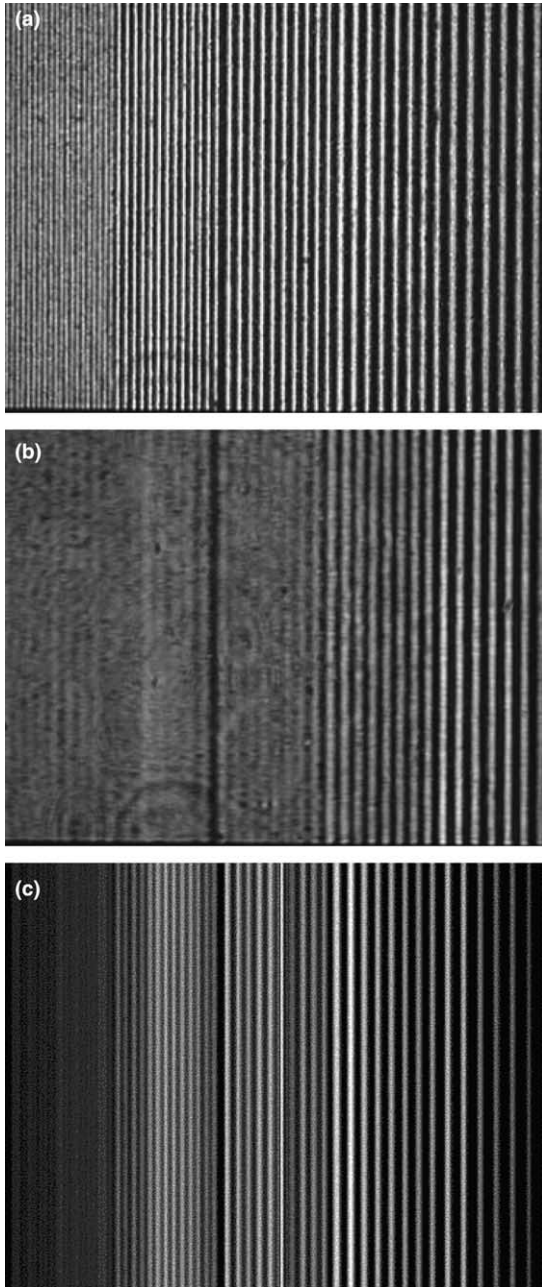


Fig. 6. Output (chirp with period ranging from 100 to 300 μm) captured by the CCD camera (a) clear aperture, (b) closed aperture without masks M and M' and (c) closed aperture with masks M and M'.

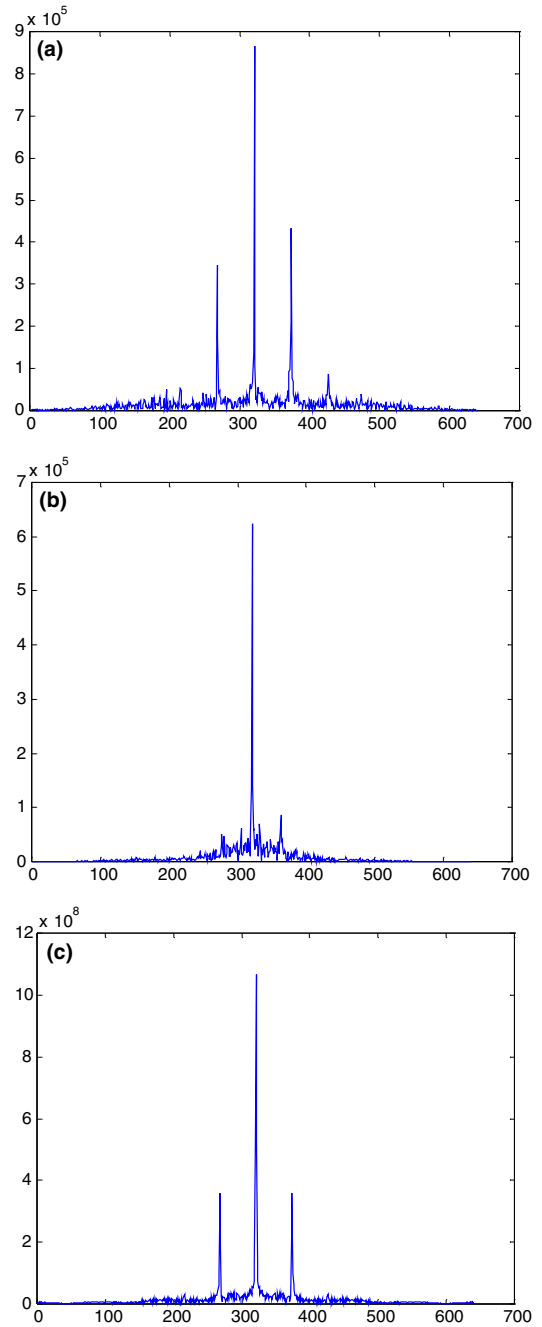


Fig. 7. The horizontal cross section of the Fourier transform (FT) of an image of a grating with period 150 μm (a) with open aperture, (b) with a closed aperture without masks M and M' and (c) a closed aperture with masks M and M'.

tracting the low resolution image (that may be obtained by capturing the picture of the original input without the super resolving mask, or by low pass filtering the spectrum of the captured super resolved image). As can be seen a better contrast was achieved with image processing. Figs. 6(a)–(c) are the results for another input (chirp with period ranging from 100 to 300 μm): The original object, the object imaged through the low pass filter and the object obtained after super resolution aided by image enhancement. Figs. 7(a)–(c) are examples of the cross section of the spatial frequency domain of a Ronchi grating with period of 200 μm with and without superresolution, the reconstruction of the high frequencies is clearly seen. The obtained results illustrate a significant improvement in the imaging ability of the system as can be seen from the comparison between Figs. 7(b) and (c). The spatial frequencies existing in Fig. 7(a) that did not pass through the system (as seen in Fig. 7(b)) were reconstructed using the super resolving approach in Fig. 7(c). The applied digital processing for obtaining the spectrum of Fig. 7(c) was subtraction of the bright line in the origins of the captured image.

5. Conclusions

In this paper, a new approach for one-dimensional superresolution that is based on spectral

dilation was introduced, this approach was experimentally demonstrated for one-dimensional gratings with varying periods. Obviously, this approach could be used for any kind of one-dimensional objects as well, or for objects with cigar shaped area in the frequency domain. It was shown both theoretically and experimentally that the high spatial frequencies that could not pass through the closed aperture of the imaging system were reconstructed using the presented approach.

Acknowledgement

Javier Garcia acknowledges the support of the Spanish Ministerio de Ciencia y Tecnologia, under the project BFM2001-3004.

References

- [1] M. Françon, *Nouvo Climento Suppl.* 9 (1952) 283.
- [2] W. Lukosz, *JOSA* 57 (1967) 932.
- [3] D. Mendlovic, A.W. Lohmann, N. Konforti, I. Kiryuschev, Z. Zalevsky, *Appl. Opt.* 36 (1997) 2353.
- [4] A.W. Lohmann, D.P. Paris, *Appl. Opt.* 3 (1964) 1037.
- [5] A.I. Kartashev, *Opt. Spectra* 9 (1960) 204.
- [6] M.A. Grimm, A.W. Lohmann, *JOSA* 56 (1966) 1151.
- [7] W. Lukosz, *JOSA* 56 (1966) 1463.
- [8] G. Toraldo Di Francia, *JOSA* 59 (1969) 799.